Conjugated Polymer Covalently Modified Multiwalled Carbon Nanotubes for Optical Limiting

LIJUAN NIU,[1] PEIPEI LI,[1] YU CHEN,[1] JUN WANG,[2] JINJUAN ZHANG,[1] BIN ZHANG,[1] WERNER J. BLAU[2]

[1]Key Laboratory for Advanced Materials, Department of Chemistry, East China University of Science and Technology, 130 Meilong Road, Shanghai 200237, China

[2]Materials Ireland Polymer Research Center, School of Physics and the Centre for Research on Adaptative Nanostructures and Nanodevices (CRANN), Trinity College Dublin, Dublin 2, Ireland

Received 29 August 2010; accepted 26 September 2010
DOI: 10.1002/pola.24423
Published online 18 November 2010 in Wiley Online Library (wileyonlinelibrary.com).

ABSTRACT: A new soluble multiwalled carbon nanotubes (MWNTs) covalently functionalized with conjugated polymer PCBF, in which the wt % of MWNTs is approximately calculated as 7.3%, and the average thickness of PCBF covalently grafted onto MWNTs is 10.4 nm, was synthesized by an amidation reaction. In contrast to the starting polymer PCBF-NH_2, grafting of PCBF onto MWNTs led to a 0.3 eV red-shift of the N1s XPS peak at 399.7 eV assigning to N in the unreacted NH_2 moieties in the resulting copolymer structure and an appearance of new peak at 402 eV corresponding to N bound to the carbonyl C (i.e., NH—C=O). Unlike PCBF-NH_2, which only displayed a weak optical limiting response at 532 nm, Z-scan for MWNT-PCBF exhibited a much broader reduction in transmission and a scattering accompanying on the focus of the lens at both 532 and 1064 nm, indicating a prominent broadband optical limiting response. The thermally induced nonlinear scattering is responsible for the optical limiting. © 2010 Wiley Periodicals, Inc. J Polym Sci Part A: Polym Chem 49: 101–109, 2011

KEYWORDS: conjugated polymer; covalent functionalization; multiwalled carbon nanotubes; NLO; optical limiting; Z-scan

INTRODUCTION

The chemistry of one-dimensional carbon nanotubes (CNTs) has been at the center of a significant research effort due to its outstanding optical, mechanical, electronic, and thermal properties.[1] The covalent attachment of appropriate chemical functional groups onto the π-conjugated skeleton of CNTs is anticipated to facilitate applications development by improving solubility and easy of dispersion and providing for chemical attachment to surfaces and polymer matrices.[2] Polymer grafting to CNTs, which has mainly been achieved on acid-treated nanotubes,[3] produces continuous advances and novel functional materials with interesting applications because of the great promise of polymers in photonics and optoelectronics. Our current interest in this area mainly involves the design and synthesis of soluble CNTs covalently functionalized with conjugtated polymers, which can be used to protect against laser radiation exposure.[4] Optical limiting is an important application of nonlinear optics, useful for the protection of human eyes, optical elements, and optical sensors from intense laser pulses. Some solube polymer-modified CNTs [including single-walled CNTs and multiwalled CNTs (MWNTs)] for optical limiting have been reported.[5] In these materials, besides nonlinear scattering, other mechanisms such as nonlinear absorption and electronic absorption may contribute to the optical limiting efficiency.[4(a)]

Here, we first synthesized a new conjugated polymer PCBF with pendent amino groups in the polymer sidechains by the Suzuki coupling reaction, as shown in Scheme 1, and then, this polymer was used to react with MWNTs with surface-bonded acryl chloride moieties to give a soluble donor–acceptor type MWNT-PCBF hybrid material in which PCBF was chosen as electron donor, whereas the MWNT itself may serve as the electron acceptor. Compared with the PCBF polymer, MWNT-PCBF exhibited excellent broadband optical limiting performance at both 532 and 1064 nm.

EXPERIMENTAL

All chemicals were purchased from Aldrich and used without further purification. To ensure the commercially available highly purified nitrogen is very dry and oxygen free, before use, it was further purified by in turn passage through three glass columns filled with anhydrous silica gel, dry 4A-zeolite, and active silver molecular sieve, respectively, to remove a trace of moisture and the possible remained oxygen in nitrogen gas.

Organic solvents used in this study were purified, dried, and distilled under dry nitrogen. The MWNTs, with a diameter of 10–20 nm, a length of 5–15 μm, and a >95% purity as well, were purchased from Tsinghua Nano-Powder Engineering

Correspondence to: Y. Chen (E-mail: chentangyu@yahoo.com) or J. Wang (E-mail: jwangsci@gmail.com)

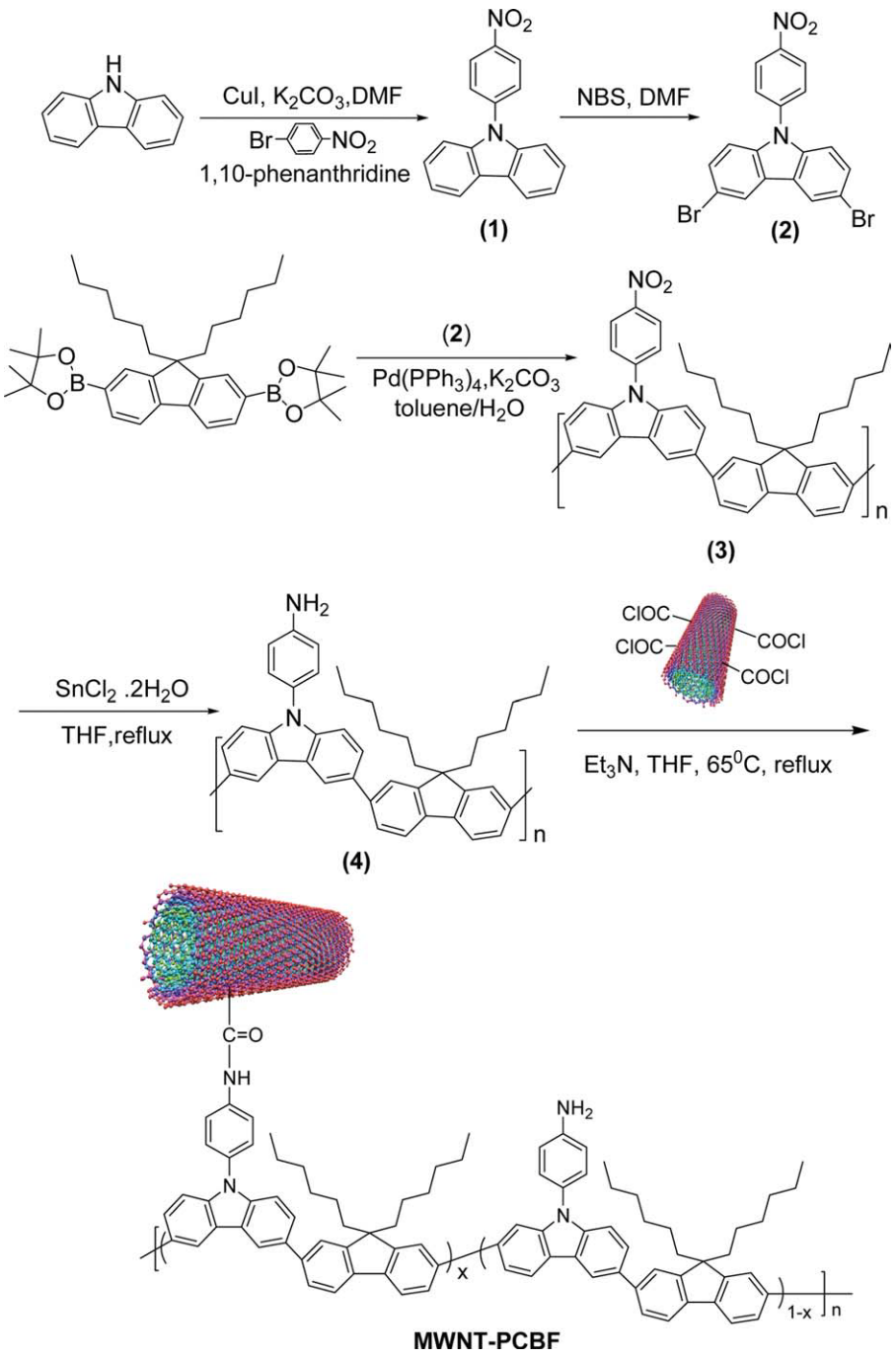

SCHEME 1 Synthesis of MWNT-PCBF hybrid material. [Color figure can be viewed in the online issue, which is available at wileyonlinelibrary.com.]

Centre (Beijing, China). The operations for synthesis before the termination reaction were carried out under purified dry nitrogen.

The ultraviolet/visible (UV/vis) absorption spectral measurements were carried out with a Shimadzu UV-2450 spectrophotometer. Thermal properties of the samples were measured using a Perkin-Elmer Pyris 1 thermogravimetric analyzer (TGA) in flowing (100 mL min^{-1}) N_2. Transmission electron microscopy (TEM) images were recorded on a JEM-2100S TEM system operated at 100 kV. Molecular weights [number-average (M_n) and weight-average (M_w)] were determined with a Waters 2690 gel permeation chromatography (GPC) using linear polystyrene standards eluting with tetrahydrofuran (THF). Steady-state fluorescence spectra were measured on a HORIBA JOBIN YVON Fluoromax-4 spectrofluorometer. The sample for the fluorescence measurement was dissolved in the dry THF, filtered, transferred to a long quartz cell, and then capped and bubbled with high pure argon (without O_2 and moisture) for at least 15 min before measurement. The absolute photoluminescence quantum yields were measured by integrating sphere method.[6] X-ray photoelectron spectroscopy (XPS) measurements were

carried on Thermo ESCALAB 250 spectrometer with a monochromatized Al KR X-ray source (1486.6 eV photons) at a constant dwell time of 100 ms and a pass energy of 20 eV. Raman spectra were taken at room temperature with a MicroRaman System RM3000 spectrometer and an argon ion laser operating at a wavelength of 514.5 nm as the excitation source.

The Z-scan technique is a well-known method to characterize the nonlinear optical (NLO) properties of materials, including nonlinear absorption, scattering, or refraction. A standard open aperture Z-scan setup was used to measure the NLO coefficients of MWNT-PCBF dispersions. This measures the total transmittance through the sample as a function of incident laser intensity while the sample is gradually moved through the focus point of a lens (along the *z*-axis). All experiments described in this article were performed with 6 ns pulses from a Q-switched Nd:YAG laser. The beam was spatially filtered to remove higher order modes and tightly focused using a 9-cm focal length lens. The laser was operated at the fundamental 1064 nm and its second harmonic, 532 nm, with a pulse repetition rate of 10 Hz. All samples were prepared by dissolving the materials in organic solvent with a concentration of 1.0 g/L, followed by gentle agitation for ~30 min in a low-power (60 W) sonic bath to ensure complete and uniform dispersal. The final dispersions were introduced into 1.0 mm quartz cells for Z-scan measurements. Linear extinction coefficients, α_0, as defined by $T = \exp(-\alpha_0 L)$ were measured for the samples, where T defines the ratio of transmitted to incident laser light, and $L = 1.0$ mm is the sample thickness. The α_0 values of the 1.0 g/L dispersions are 4.10 cm^{-1} at 532 nm and 6.61 cm^{-1} at 1064 nm, which corresponds to a linear transmission T of 66.4 and 51.6%, respectively.

Synthesis of 9-(4-Nitrophenyl)-9*H*-Carbazole (1)

A stirred DMF solution of 1-bromo-4- nitrobenzene (14.47 g, 72 mmol), carbazole (10.02 g, 60 mmol), K_2CO_3 (8.29 g, 60 mmol), 1,10-phenanthridine (2.16 g,12 mmol), and CuI (2.27 g,12 mmol) was heated at 155°C for 24 h. After cooling down to room temperature, 500 mL of ice-water was poured into the reaction mixture. The collected yellow soild was washed with distilled water and anhydrous methanol for several times, respectively, and dried at 50°C for 6 h under reduced pressure. Yield: 15 g (88%). ^{1}H NMR ($CDCl_3$, 500 MHz): δ/ppm = 8.46 (m, 2H), 8.14 (d, 2H, J = 8 Hz), 7.78 (m, 2H), 7.49 (d, 2H, J = 8 Hz), 7.44 (m, 2H), 7.34 (m, 2H); EI-MS: m/z 288.1[M^+].

Synthesis of 3,6-Dibromo-9-(4-nitrophenyl)-9H-Carbazole (2)

9-(4-nitrophenyl)-9H-carbazole (8.67 g, 30 mmol) and *N*-bromosuccinimide (NBS, 11.74 g, 66 mmol) was stirred in anhydrous dimethylformamide (50 mL) at 0 °C for 48 h, and then to the above system was added 500 mL of ice-water. The collected yellow precipitate was washed with water and methanol for several times, respectively, and dried at 50 °C for 6 h under reduced pressure. Yield: 10 g (75%). ^{1}H NMR ($CDCl_3$, 500 MHz): δ/ppm = 8.51–8.49 (m, 2H), 8.21 (d, 2H), 7.76–7.73 (m, 2H), 7.57–7.54 (m, 2H), 7.34–7.32 (d, 2H). EI-MS: m/z 445.9 [M^+].

PCBF with Pendent NO_2 Groups (3)

To a mixture of 3,6-dibromo-9-(4-nitrophenyl)-9H-carbazole (624 mg, 1.4 mmol), 9,9-dihexylfluorene-2,7-bis(4,4,5,5-tetramethyl-1,3,2-dioxa-borolane) (815 mg, 1.4 mmol), $Pd(PPh_3)_4$ (32 mg), and K_2CO_3 (1100 mg) was added a mixture of toluene and water (v/v 2:1). After vigorously stirring at 90 °C for 48 h, the reaction mixture was allowed to cool to room temperature and then poured into a stirred MeOH/H_2O solution (v/v 10:1) and filtered to give a yellow solid, which was subsequently washed with MeOH and water, followed by MeOH again. The collected crude product was extracted with acetone (200 mL) for 2 days in a Soxhlet apparatus to remove oligomers and catalyst residues. The residual solid in the thimble was dried to give 690 mg of yellow solid. ^{1}H NMR ($CDCl_3$): δ/ppm = 8.54 (m, 2H, Ar), 7.71 (m, 12H, Ar), 6.99 (m, 2H, Ar), 2.12 (m, 4H, CCH_2), 1.11 (m, 12H, $6CH_2$), 0.78 (m, 10H, $2CH_2CH_3$).

Synthesis of PCBF-NH_2 (4)

To a solution of polymer **3** (500 mg) in 50 mL of THF was added quickly 96 wt % $SnCl_2$-$2H_2O$ (910 mg) and then heated under reflux for 24 h. After removal of most of the THF under reduced pressure, to the reaction mixture was added saturated aq. NaOH solution dropwisely with stirring until the liquid became alkaline. The product was extracted with chloroform. The combined organic layers was dried over anhydrous $MgSO_4$, and filtered. After evaporation of the solvent, the product was redissolved in THF and then reprecipitated from MeOH to give 360 mg of yellow polymer. ^{1}H NMR ($CDCl_3$, 500 MHz): δ/ppm = 8.39 (m, 2H, Ar), 7.49 (m, 12H, Ar), 6.94 (m, 2H, Ar), 3.83 (s, 2H, NH_2), 2.02 (m, 4H, CCH_2), 1.04 (m, 12H, $6CH_2$), 0.70 (m, 10H, $2CH_2CH_3$). GPC: $M_n = 3.6 \times 10^3$, Pd = 1.14. Its optimized three-dimensional structure was shown in Figure 1.

Synthesis of MWNT-COCl

A total of 5.0 g of crude MWNTs were marinated in 38% HCl for 1 day, filtered, and washed with deionization water until neutral. A mixture of MWNTs, HNO_3 (30 mL, 60%), and H_2SO_4 (90 mL, 98%) was first sonicated at 40 °C for 30 min and then was refluxed 2 h. After termination of reaction, it was allowed to cool down to room temperature. The mixture was diluted with a large amount of deionized water, followed by a vacuum-filtering through a Nylon film (ϕ0.45 μm). The obtained solid, in which polar carboxyl groups were introduced into the convex surface of MWNTs, was washed with water until the aqueous layer reached neutral and then was vacuum-dried at 60 °C for 3 h. The COOH-containing MWNTs (3.7 g) were reacted with a large excess of $SOCl_2$ containing a catalytic amount of *N,N*-dimethylformamide under reflux for 24 h. After centrifugation, the remaining solid was washed with anhydrous THF to remove the residual thionyl chloride. The obtained MWNT-COCl was kept in dry nitrogen.

Synthesis of MWNT-PCBF

To a suspension of MWNT-COCl (150 mg) in anhydrous THF (40 mL) was added PCBF-NH_2 (300 mg) and Et_3N (5 mL)

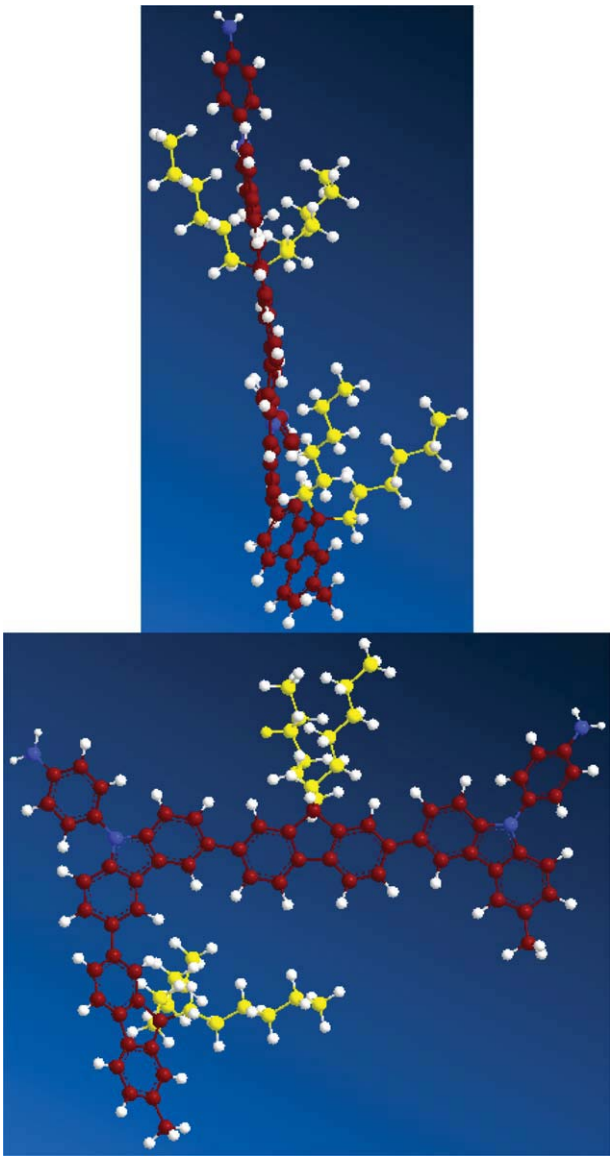

FIGURE 1 Optimized structure of PCBF-NH_2 (red: carbon atoms in main chain; yellow: carbon atoms in side chain; blue: nitrogen atoms; white: hydrogen atoms). The two hexyl side chains at the C-9 position of the fluorene unit are located on both sides of the plane of the polymer backbone.

under purified argon. The reaction mixture was sonicated 30 min at 40 °C first and then refluxed at 65 °C for 3 days. After cooling to room temperature and removing the solvent under reduced pressure, the solid product was washed with a large amount of water to remove the triethylammonium salts formed during the reaction and then redispersed in 100 mL of THF. The obtained solution was vacuum-filtered through a single layer polytetrafluor ethylene film (ϕ0.45 μm) until the filtration being colorless to remove the unreacted polymer. The black solid on the film was collected and then was well-dispersed in THF under the ultrasonic irradiation (40 KHz), followed by filtering through a three-layer-filter paper until the filtration being colorless to remove the posisble unreacted MWNTs. The polymer collected after evaporation of the solvent was washed twice with methanol and dried at 60 °C *in vacuum* for 10 h. Yield: 215 mg.

RESULTS AND DISCUSSION

Covalent graftings of PCBF onto the MWNTs surface considerably improved the solubility of MWNTs, as shown in Figure 2. The solubility of the MWNT-PCBF in organic solvents is mainly dependent on the percentage of polymer grafted onto MWNTs. As contrast, it is very difficult to well-disperse MWNTs into any organic solvent, even if under ultrasonic irradiation. From Figure 3, it can be clearly seen that the average diameter of MWNT-COOH is about 14.3 nm, whereas that of MWNT-PCBF increases to 35 nm. This result implies that the average thickness of PCBF covalently grafted onto MWNTs is 10.4 nm.

The UV/vis absorption of PCBF-NH_2 in THF (Fig. 4) displayed a strong peak at 340 nm and a shoulder peak at 318 nm. There is no obvious linear absorption at wavelength range longer than 400 nm. In contrast to PCBF-NH_2, the absorption spectrum of MWNT-PCBF was slightly shifted to the blue relative to the former due to the possible intermolecular and intramolecular charge transfer in the system and exhibited an absorbance decreased gradually in the range of 400–550 nm, which is typical electronic absorption characteristics of solubilized CNT.[7] Upon excitation of 375 nm laser, the photoluminescence intensity of MWNT-PCBF significantly decreased when compared with that of PCBF-NH_2, suggesting that the quenching process is probably due to the electron-transfer process from polymer to ^{1}MWNTs*.

The XPS provides essential and useful information for the covalent attachment of the polymer onto the surface of MWNTs (Fig. 5). The N1s XPS spectrum of PCBF-NH_2 clearly indicated that the peak of nitrogen functionality appeared at

FIGURE 2 Comparison of solubility of the samples in THF: (a) MWNTs, (b) MWNT-COOH, and (c) MWNT-PCBF. The black dispersion shown in (c) is stable for at least 1 month. The concentration for each sample is 5 mg/mL.

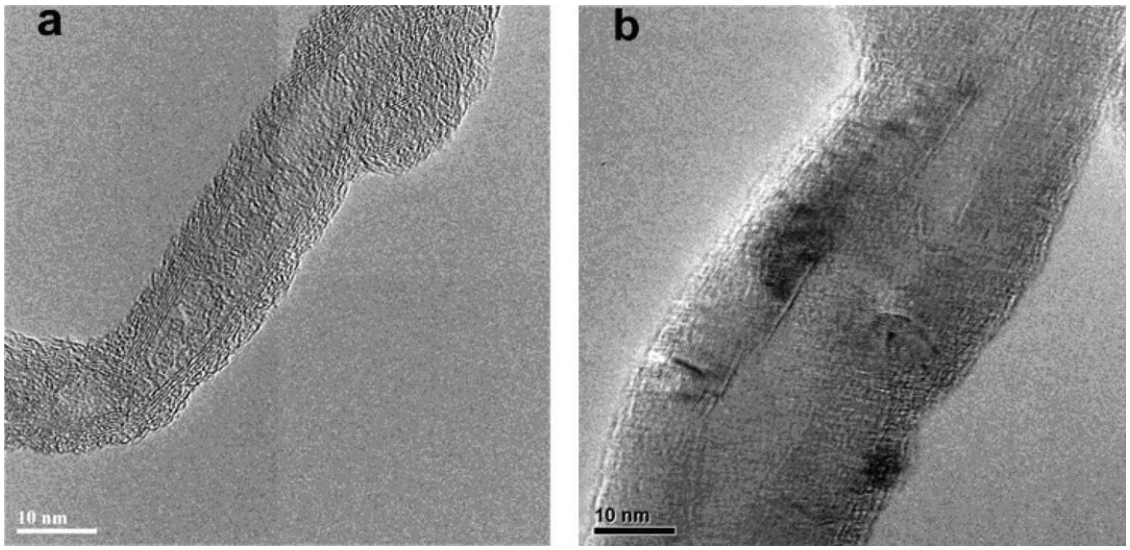

FIGURE 3 TEM images of (a) MWNT-COOH and (b) MWNT-PCBF.

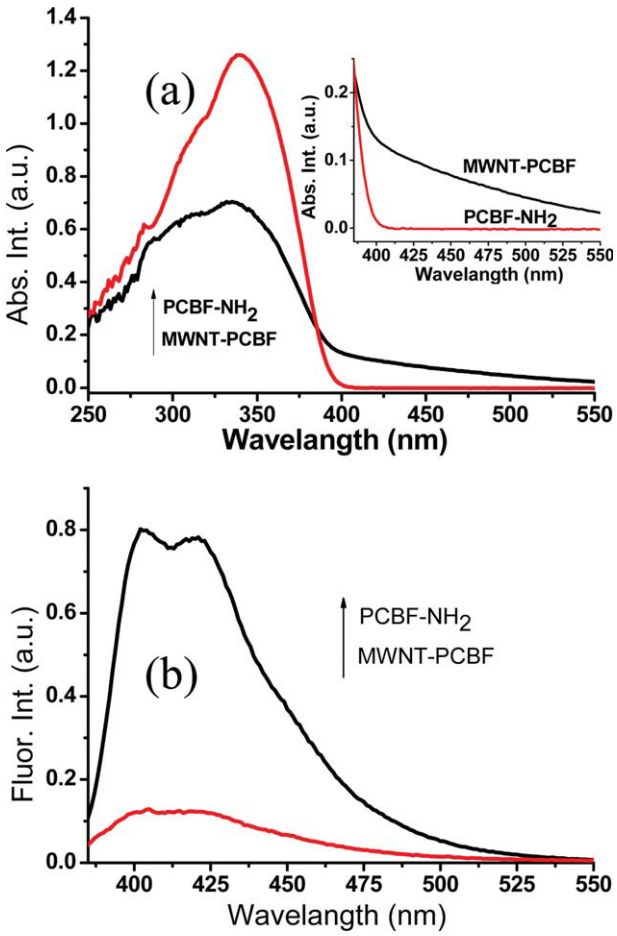

FIGURE 4 (a) UV/vis absorption and (b) photoluminescence (λ_{ex} = 375 nm) spectra of the samples in dilute THF solution. [Color figure can be viewed in the online issue, which is available at wileyonlinelibrary.com.]

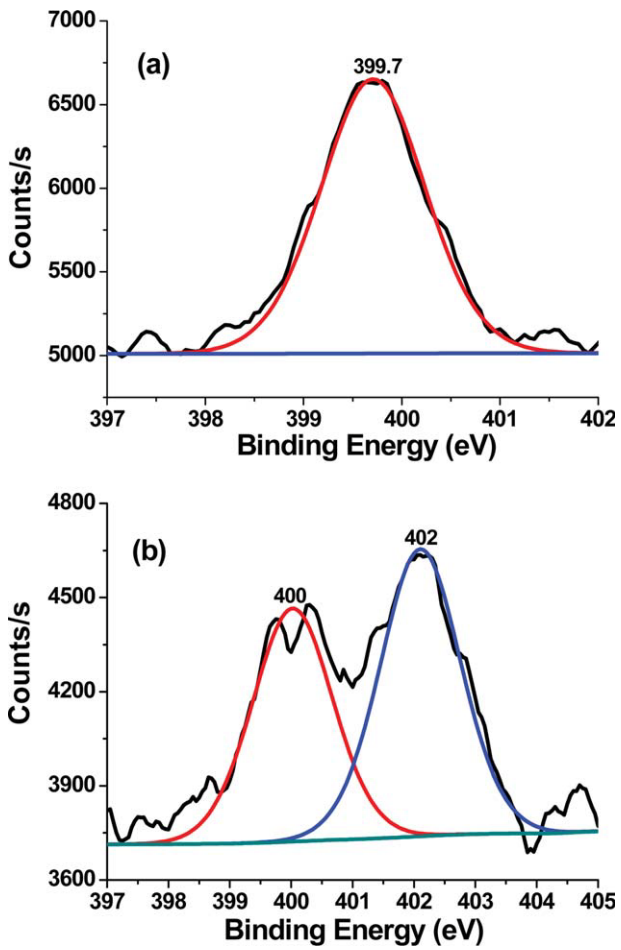

FIGURE 5 The N1s XPS spectra of (a) PCBF-NH_2 and (b) MWNT-PCBF. [Color figure can be viewed in the online issue, which is available at wileyonlinelibrary.com.]

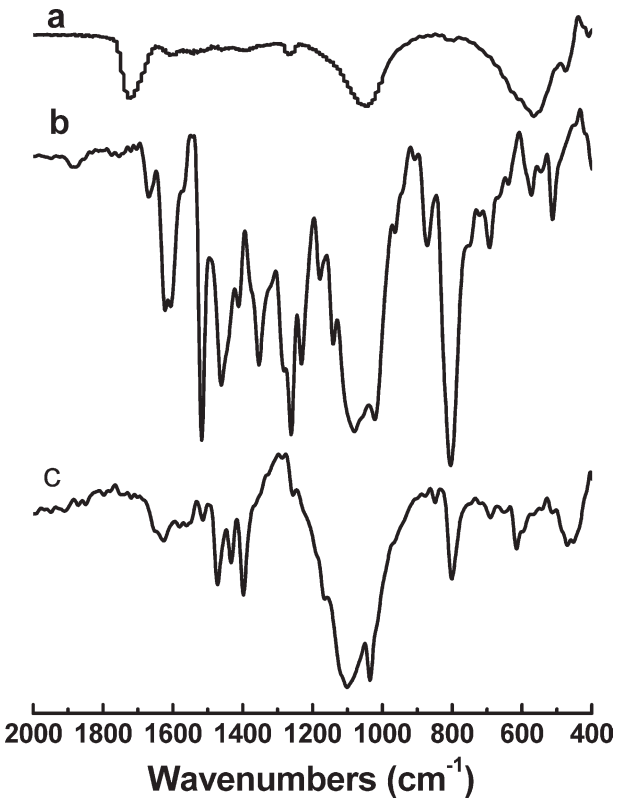

FIGURE 6 FTIR spectra of (a) MWNT-COOH, (b) PCBF-NH_2, and (c) MWNT-PCBF.

399.7 (the N in —NH_2). In contrast to the polymer reference, covalent grafting of PCBF onto MWNTs led to a 0.3 eV red-shift of the peak assigning to N in the unreacted NH_2 moieties in the resulting polymer structure, and an appearance of new peak at 402 eV corresponding to N bound to the carbonyl C (i.e., NH—C=O). The formation of an amido bond between MWNT and polymer was also confirmed by FTIR spectroscopy. The characteristic vibration for the carboxylic acid groups attached onto the surface of MWNTs was observed at 1724 cm^{-1} in the IR spectrum of MWNT-COOH, as shown in Figure 6. The spectrum of PCBF-NH_2 shows NH_2 bending mode at 1594 cm^{-1} and the C—N stretching mode at 1257 cm^{-1}. After polymer grafting onto MWNTs, the stretching mode of an amido bond at 1658 cm^{-1} ($\nu_{NH—C=O}$) was detected in the IR spectrum of MWNT-PCBF.

Basically, the actual amount of C_{60} incorporated in the polymer can be determined by thermogravimetric analysis (TGA).[8] Followed this idea, we determined the amount of MWNTs in MWNT-PCBF by using similar method. As shown in Figure 7, MWNTs are stable over a wide temperature range. At 700 °C only 1.4% weight loss was observed due to the possible organic and inorganic impurities trapped in MWNTs. In contrast, the acid-functionalized MWNTs (i.e., MWNT-COOH) are less thermally stable perhaps due to the defects on the nanotube surface caused by the acid etching. The TGA curve of MWNT-COOH exhibited a rapid mass loss of 13.5% between 100 and 400 °C, followed by a very slow

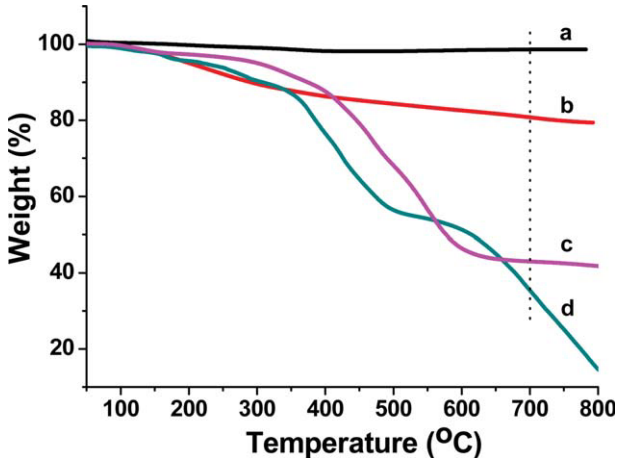

FIGURE 7 TGA curves of (a) MWNTs, (b) MWNT-COOH, (c) MWNT-PCBF, and (d) PCBF-NH_2 in flowing (100 mL min^{-1}) N_2. [Color figure can be viewed in the online issue, which is available at wileyonlinelibrary.com.]

weight loss of 5.9% up to 700 °C at which the amount of the MWNT residue is about 80.7%. By comparing the amount of the residues that these two samples left at 700 °C, the wt % of oxygen-containing groups at MWNT defect sites was estimated roughly to be about 17.9%. The thermal stability of MWNT-PCBF is apparently higher than that of PCBF-NH_2. The amounts of the MWNT-PCBF and the PCBF residues at 700 °C are 43.1 and 35.8%, respectively. By assuming that the PCBF residues remaining in the MWNT-

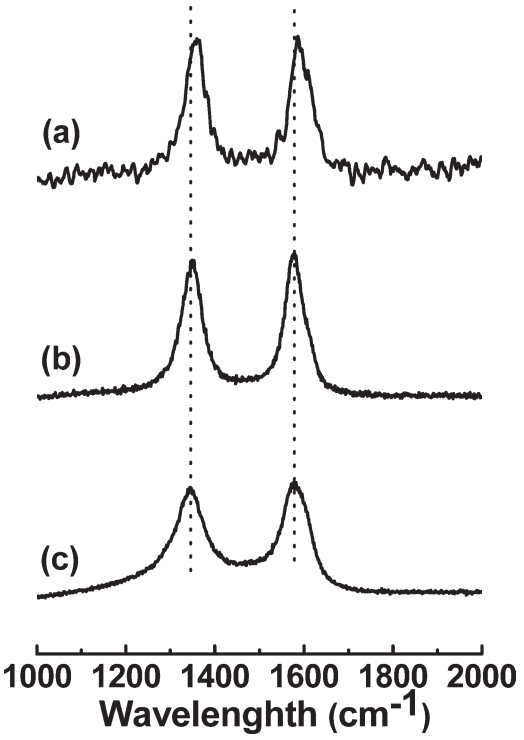

FIGURE 8 Raman spectra of (a) MWNT-PCBF, (b) MWNT-COOH, and (c) MWNTs. $\lambda_{ex} = 514.5$ nm.

TABLE 1 Linear and NLO Coefficients of MWNT-PCBF and PCBF-NH_2 in DMF at a Concentration of 1.0 g/L

Sample	λ (nm)	T (%)	α_0 (cm^{-1})	β_{eff} (cm GW^{-1})	Im $\{\chi^{(3)}\}$ ($\times 10^{-12}$, esu)
MWNT-PCBF	532	66.4	4.10	20.29 ± 0.92	6.99 ± 0.32
	1064	51.6	6.61	29.08 ± 0.89	20.04 ± 0.61
PCBF-NH_2	532	95.7	0.44	0.47 ± 0.00	0.16 ± 0.00
	1064	94.6	0.56	N.A.	N.A.

α_0: linear extinction coefficient; β_{eff}: nonlinear extinction coefficient; Im $\{\chi^{(3)}\}$:the imaginary third-order susceptibility.

PCBF hybrid material at 700 °C have the same wt % as that of PCBF-NH_2, the wt % of MWNTs in the MWNT-PCBF structure may be approximately calculated as 7.3%.

With excitation of 514.5 nm laser, the Raman spectrum of MWNTs (Fig. 8) exhibited two prominent bands at about 1341 (D-band) and 1579 (G-band) cm^{-1}.[2(a),9] The former indicates, as usual for CNT structures, the density of defects and has been used to monitor the process of covalent functionalization, which transforms sp^2 to sp^3 sites, whereas the latter could be utilized to estimate the level and distribution of modification. After acid treatment, the observed D- and G-bands appeared at 1350 and 1579 cm^{-1}, respectively, being attributed to the defects and disorder-induced modes and in-plane E_{2g} zone-center mode.[10] In contrast to MWNT-COOH, the D- and G-bands of MWNT-PCBF are shifted to the high wavenumbers by $\Delta\lambda = 12$ and 8 cm^{-1}, respectively. The D- to G-band intensity ratios (I_D/I_G) for MWNT-COOH and MWNT-PCBF are about 0.96 and 0.99, respectively.

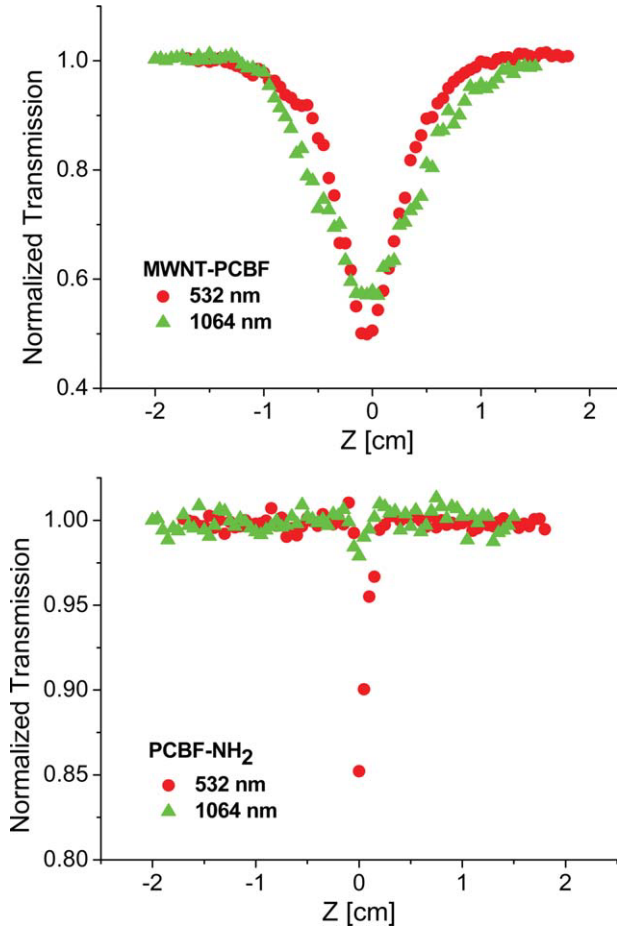

FIGURE 9 Typical open-aperture Z-scan curves for PCBF-NH_2 and MWNT-PCBF with the concentration of 1.0 mg/mL in DMF. [Color figure can be viewed in the online issue, which is available at wileyonlinelibrary.com.]

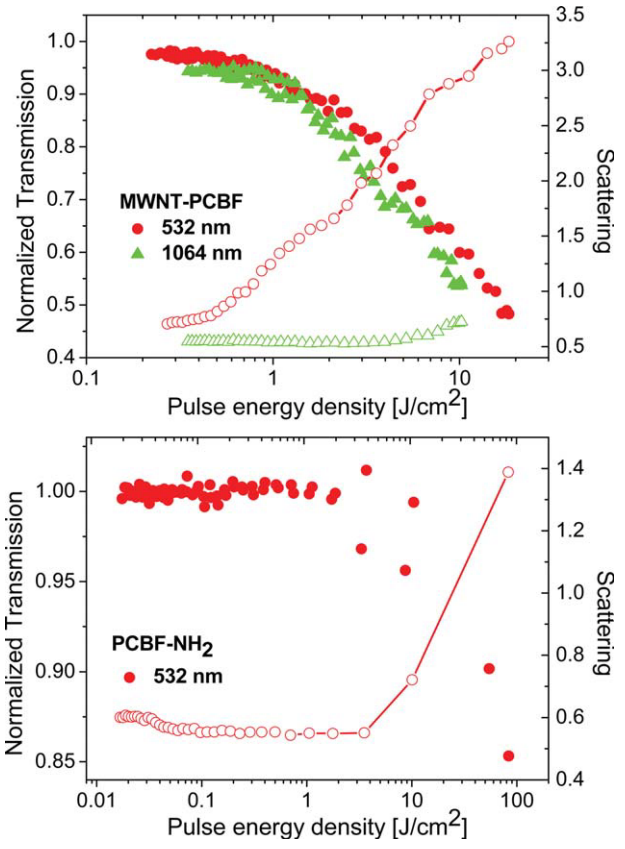

FIGURE 10 Plots of normalized transmission and scattering response against incident pulse energy density for PCBF-NH_2 and MWNT-PCBF with the concentration of 1.0 mg/mL in DMF. [Color figure can be viewed in the online issue, which is available at wileyonlinelibrary.com.]

Figure 9 shows the typical open-aperture Z-scan results for the PCBF-NH_2 and the MWNT-PCBF, respectively. Unlike PCBF-NH_2, which only displayed weak optical limiting responses at 532 nm, *Z*-scan for MWNT-PCBF exhibited a much broader reduction in transmission at both 532 and 1064 nm, indicating a prominent broadband optical limiting response. The depth of reduction usually changes along with the variations of the on-focus intensity. At the same on-focus intensity, a covalent bonding between MWNTs and PCBF resulted in the further decrease of the minimal normalized transmittance from 85.3% for PCBF-NH_2 to 49.7% for MWNT-PCBF at 532 nm. Table 1 summarizes the linear and NLO coefficients of the samples. The NLO extinction coefficient of MWNT-PCBF is 43 times that of PCBF-NH_2 at 532 nm. This value must contain the effects from light scattering, nonlinear absorption, and saturated absorption. However, we currently do not have suitable experimental setup to quantitatively analyze the contributions of the scattering and nonlinear absorption to optical limiting.

Figure 10, in which the normalized transmission and the corresponding scattering were plotted as functions of input energy density (J cm^{-2}), presents the optical limiting behavior of MWNT-PCBF and PCBF-NH_2. It can be clearly seen that MWNT-PCBF presents much better optical limiting performance than PCBF-NH_2. The MWNT-PCBF manifests the remarkable broadband optical limiting with the comparable limiting performance for both 532 and 1064 nm pulses. A lot of theoretical and experimental results have demonstrated that the optical limiting responses of CNT suspensions are shown to be dominated by nonlinear scattering as a result of thermally induced solvent-bubble formation and sublimation of the nanotubes, whereas the solubilized CNTs optically limit through nonlinear absorption mechanism and exhibit significant solution-concentration-dependent optical limiting responses.[4(a)] Therefore, we believed that the thermally induced nonlinear scattering dominated the optical limiting for ns pulses at 532 and 1064 nm. As shown in Figure 10, the big difference for the scattered intensity at 532 and 1064 nm is mainly due to the wavelength dependent response of the Si photodiode that we used to measure the scattered light. The response of the Si photodiode at 532 nm is much larger than that at 1064 nm. Although the nonlinear scattering dominates the optical limiting observed from the MWNT-PCBF dispersions, we could not rule out the possible minor contributions from nonlinear absorption or electronic absorption.

CONCLUSIONS

Polymer grafting to CNTs produces continuous advances and novel functional materials with interesting applications due to their great promise in photonics and optoelectronics. We designed and synthesized a new soluble conjugated polymer covalently grafted MWNTs hybrid material, MWNT-PCBF, by reaction of the surface-bound acryl chloride groups in MWNT-COCl with PCBF-NH_2. The wt % of MWNTs in the resulting polymer is approximately calculated as 7.3%. Upon excitation of 375 nm laser, compared with PCBF-NH_2, the photoluminescence of MWNT-PCBF was significantly quenched probably due to the electron-transfer process from polymer to ^{1}MWNTs*. Covalent attachment of PCBF onto MWNTs led to a 0.3 eV red-shift of the N1s XPS peak at 399.7 eV assigning to N in the unreacted NH_2 moieties in the resulting copolymer structure, and an appearance of new peak at 402 eV corresponding to N bound to the carbonyl C (i.e., NH—C=O). In contrast to MWNT-COOH, the D- and G-bands of MWNT-PCBF are shifted to the high wavenumbers by $\Delta\lambda = 12$ and 8 cm^{-1}, respectively. MWNT-PCBF presents much better optical limiting performance than PCBF-NH_2 at both 532 and 1064 nm. Microplasmas- and/or microbubbles-induced nonlinear scattering is considered as the main mechanism for optical limiting.

The authors are grateful for the financial support of the National Natural Science Foundation of China (20876046), the Ministry of Education of China (309013), the Fundamental Research Funds for the Central Universities, the Shanghai Municipal Educational Commission for the Shuguang fellowship (08GG10), and the Shanghai Eastern Scholarship.

REFERENCES AND NOTES

1 Tasis, D.; Tagmatarchis, N.; Bianco, A.; Prato, M. Chem Rev 2006, 106, 1106–1136.

2 (a) Bahr, J. L.; Tour, J. M. J Mater Chem 2002, 12, 1952–1958; (b) Zhang, B.; Chen, Y.; Wang, J.; Blau, W. J.; Zhuang, X. D.; He, N. Carbon 2010, 48, 1738–1742; (c) Yan, Y.; Zhao, S.; Cui, J.; Yang, S. J Polym Sci A: Polym Chem 2009, 47, 6135–6144; (d) Jeon, I. Y.; Tan, L. S.; Baek, J. B. J Polym Sci A: Polym Chem 2008, 46, 3471–3481; (e) Li, S.; Chen, H.; Bi, W.; Zhou, J.; Wang, Y.; Li, J.; Cheng, W.; Li, M.; Li, L.; Tang, T. J Polym Sci A: Polym Chem 2007, 45, 5459–5469; (f) Hong, C. Y.; You, Y. Z.; Pan, C. Y. J Polym Sci A: Polym Chem 2006, 44, 2419–2427; (g) Pei, X.; Liu, W.; Hao, J. J Polym Sci A: Polym Chem 2008, 46, 3014–3023; (h) Shanmugharaj, A. M.; Bae, J. H.; Nayak, R. R.; Ryu, S. H. J Polym Sci A: Polym Chem 2007, 45, 460–470; (i) Narain, R.; Housni, A.; Lane, L. J Polym Sci A: Polym Chem 2006, 44, 6558–6568.

3 (a) Sano, M.; Kamino, A.; Okamura, J.; Shinkai, S. Langmuir 2001, 17, 5125–5128; (b) Hill, D. E.; Lin, Y.; Rao, A. M.; Allard, L. F.; Sun, Y. Macromolecules 2002, 35, 9466–9471; (c) Kumar, N. A.; Kim, S. H.; Cho, B. G.; Lim, K. T.; Jeong, Y. T. Colloid Polym Sci 2009, 287, 97–102; (d) Baskaran, D.; Sakellariou, G.; Mays, J. W.; Bratcher, M. S. J Nanosci Nanotechnol 2007, 7, 1560–1567; (e) Liu, Y. X.; Du, Z. J.; Li, Y.; Zhang, C.; Li, H. Q. Chin J Chem 2006, 24, 563–568.

4 (a) Chen, Y.; Lin, Y.; Liu, Y.; Doyle, J.; He, N.; Zhuang, X.; Bai, J.; Blau, W. J. J Nanosci Nanotechnol 2007, 7, 1268–1283; (b) Wang, J.; Chen, Y.; Blau, W. J. J Mater Chem 2009, 19, 7425–7443.

5 (a) Riggs, J. E.; Walker, D. B.; Carroll, D. L.; Sun, Y. P. J Phys Chem B 2000, 104, 7071–7076; (b) Menna, E.; Scorrano, G.; Maggini, M.; Cavallaro, M.; Della, N. F.; Battagliarin, M.; Bozio, R.; Fantinel, F.; Meneghetti, M. Arkivoc 2003, 12, 64–73; (c) Li,

C.; Liu, C.; Li, F.; Gong, Q. Chem Phys Lett 2003, 380, 201–205; (d) Yi, W. H.; Feng, W.; Xu, Y. L.; Wu, H. C. Jpn J Appl Phys (Part 1) 2005, 44, 3022–3027; (e) Feng, W.; Yi, W.; Wu, H.; Ozaki, M.; Yoshino, K. J Appl Phys 2005, 98, 034301/1–034301/7; (f) Zhang, B.; Wang, J.; Chen, Y. ; Früchtl, D.; Yu, B.; Zhuang, X.; He, N.; Blau, W. J. J Polym Sci A: Polym Chem 2010, 48, 3161–3168.

6 Porrès, L.; Holland, A.; Pålsson, L. O.; Monkman, A. P.; Kemp, C.; Beeby, A. J Fluoresc 2006, 16, 267–272.

7 Wu, H. X.; Tong, R.; Qiu, X. Q.; Yang, H. F.; Lin, Y. H.; Cai, R. F.; Qian, S. X. Carbon 2007, 45, 152–159.

8 Chen, Y.; Huang, Z. E.; Cai, R. F. J Polym Sci B: Polym Phys 1996, 34, 631–640.

9 (a) Ballesteros, B.; de la Torre, G.; Ehli, X.; Rahman, G. M. A.; Agullo-Rueda, F.; Guld, D. M.; Torres, T. J Am Chem Soc 2007, 129, 5061–5068; (b) Gao, C.; Jin, Y. Z.; Kong, H.; Whitby, R. L. D.; Acquah, S. F. A.; Chen, G. Y.; Qian, H.; Hartschuh, A.; Silva, S. R. P.; Henley, S.; Fearon, P.; Kroto, H. W.; Walton, D. R. M. J Phys Chem B 2005, 109, 11925–11932; (c) Guo, Z.; Du, F.; Ren, D.; Chen, Y.; Zheng, J.; Liu, Z.; Tian, J. J Mater Chem 2006, 16, 3021–3030.

10 Hamon, M. A.; Chen, J.; Hu, H.; Chen, Y.; Itkis, M. E.; Rao, A. M.; Eklund, P. C.; Haddon, R. C. Adv Mater 1999, 11, 834–840.